Iraqi National Journal of Earth Science

www.earth.uomosul.edu.iq

Integrated Geospatial Analysis of Geomorphometric Characteristics in the Hasab Watershed's Drainage Network, Iraqi Southern Desert

Bashar F. Maaroof [1*], Hashim H. Kareem [2], Jaffar H. Al-Zubaydi [3], Manal Sh. Al-Kubaisi [4], Ban AL- Hasani [5], Mawada Abdellatif [6], Iacopo Carnacina [7]

[1] *Babylon Center for Civilization and Historical Studies, University of Babylon, Hillah, Babil, Iraq.*
[2] *Department of General Sciences, University of Misan, Amarah, Misan, Iraq.*
[3] *Department of Applied Geology, University of Babylon, Hillah, Babil, Iraq.*
[4] *Department of Geology, University of Baghdad, Baghdad, Iraq.*
[5,6,7] *Civil Engineering and Built Environment Department, Faculty of Engineering Technology, Liverpool John Moores University, Liverpool L3 5UX, UK.*

Article information

Received: 10- Feb -2025

Revised: 29- Mar -2025

Accepted: 31- May -2025

Available online: 01-Apr – 2026

Keywords:
Fluvial Geomorphology,
Geomorphometry,
Watershed Modeling,
Hasab Watershed (HWS),

Correspondence:
Name: Bashar F. Maaroof

Email:
basharma@uobabylon.edu.iq

ABSTRACT

The geomorphometric characteristics of the Hasab catchment in the Iraqi southern desert are studied. The study utilized geospatial data, including the Digital Elevation Model (DEM) (SRTM), satellite imagery, and topographic maps, to analyze the geomorphometric characteristics of a watershed and then incorporated them into a topological model. The order priorities were ranked from 2677 to 167, with percentages of 35.316%, 23.245%, 16.596%, 11.728%, 10.910%, and 2.2031. The Hasab watershed has 4342.563 km of stream length, with Hasab sub-watershed (1) accounting for 50.882% and Hasab sub-watershed (4) 28.045% having the second-most length. The bifurcation ratios of sub-watersheds vary based on geological and climatic data, with the highest ratio in the Hasab sub-watershed at 10.235, followed by others at 2.151, 2.318, and 1.263. The Hasab watershed's stream frequency is 1.421 km/km2, with sub-watershed rates increasing to 2.126 km/km2. Sub-watershed values range from 2.958 km/km2 to 1.252 km/km2. The Hasab watershed has a drainage density of 1.387 km/km2, with sub-watersheds having varying density values. The highest density is 1.392 km/km2 in Hasab sub-watershed (4), while the lowest is 0.716 km/km2 in Hasab sub-watershed (3). The Hasab watershed has a basin texture rate of 11.290 Stream/km, with the highest value in Hasab sub-watershed (4) and the lowest in Hasab sub-watershed (2). Factors like basin area, rock formation hardness, structural features, rainfall intensity, slopes, basin shape, and vegetation density influence stream order diversity in basins. Waterway length rates and bifurcation ratios vary, with first-order streams transitioning into second-order ones due to river captivity.

DOI: 10.33899/injes.v26i2.60866,

التحليل الجيومكاني المتكامل للخصائص الجيومورفومترية لشبكة التصريف النهري لمستجمع مياه حسب في الصحراء العراقية الجنوبية

بشار معروف [1*] ، هاشم كريم [2] ، جعفر الزبيدي [3] ، منال الكبيسي [4] ، بان الحسني [5] ، مودة عبداللطيف [6] ، ياكوبو كارناسينا [7]

[1] مركز بابل للدراسات الحضارية والتاريخية، جامعة بابل، الحلة، بابل، العراق.

[2] قسم العلوم العامة، جامعة ميسان، العمارة، ميسان، العراق.

[3] قسم علوم الأرض التطبيقية، جامعة بابل، الحلة، بابل، العراق.

[4] قسم علوم الأرض، جامعة بغداد، بغداد، العراق.

[7،6،5] قسم الهندسة المدنية والبيئة المبنية، كلية تكنولوجيا الهندسة، جامعة ليفربول جون موريس، ليفربول L3 5UX ، المملكة المتحدة.

معلومات الارشفة

تاريخ الاستلام: 10- فبراير -2025

تاريخ المراجعة: 29- مارس -2025

تاريخ القبول: 31- مايو -2025

تاريخ النشر الالكتروني: 01- ابريل -2026

الكلمات المفتاحية:

الجيومورفولوجيا النهرية،

الجيومورفومتري،

نمذجة الاحواض النهرية،

مستجمع مياه حسب،

المراسلة:

الاسم: بشار معروف

Email: basharma@uobabylon.edu.iq

الملخص

تناول البحث دراسة الخصائص الجيومورفومترية لشبكة التصريف النهري لمستجمع مياه حسب في صحراء العراق الجنوبية. استخدمت الدراسة البيانات الجيومكانية من خلال نموذج الارتفاع الرقمي (SRTM) (DEM) وصور الأقمار الصناعية والخرائط الطبوغرافية لتحليل الخصائص الجيومورفومترية للمستجمع المائي ودمجها في نموذج طوبولوجي. تراوحت المراتب النهرية من167 إلى 2677 ، بنسب 35.316٪، 23.245٪، 16.596٪، 11.728٪، 10.910٪، و 2.2031% على التوالي. بلغت أطول المجاري النهرية لمستجمع مياه حسب الرئيس 4342.563 كم، حيث يمثل مستجمع مياه حسب الثانوي (1) 50.882٪ ومستجمع مياه حسب الثانوي (4) (28.045٪) وهو ثاني أطول مجرى مائي. تباينت نسب التفرع في مستجمعات المياه الثانوية، وذلك حسب تأثير العوامل الجيولوجية والمناخية، حيث بلغت 10.235 في مستجمع مياه حسب الثانوي (4) وهي أعلى نسبة. بلغ معدل التكرار النهري لمستجمع مياه حسب الثانوي (4)1.421 كم/كم^2، مع زيادة معدلات مستجمعات المياه الثانوية إلى 2.126 كم/كم^2، وقد تراوحت بقية القيم من 2.958 كم/كم^2 إلى 1.252 كم/كم^2. بلغت كثافة التصريف لمستجمع مياه حسب الرئيس 1.387 كم/كم^2، مع وجود قيم كثافة متفاوتة لمستجمعات المياه الفرعية، أعلى كثافة هي 1.392 كم/كم^2 في مستجمع مياه حسب الثانوي (4)، بينما أدنى كثافة هي 0.716 كم/كم^2 في مستجمع مياه حسب الثانوي (3). بلغ معدل النسيج الحوضي 11.290 مجرى مائي/كم، مع أعلى قيمة في مستجمع المياه حسب الثانوي (4) وأدنى قيمة في مستجمع المياه حسب الثانوي (2). تؤثر عوامل مثل مساحة الحوض، وصلابة تكوين الصخور، والخصائص التركيبية، وكثافة هطول الأمطار، والمنحدرات، وشكل الحوض على تنوع ترتيب المجاري المائية في الأحواض. تتنوع معدلات طول المجاري المائية ونسب التفرع، مع انتقال المجاري المائية من الدرجة الأولى إلى مجاري من الدرجة الثانية بسبب أسر النهر.

DOI: 10.33899/injes.v26i2.60866, ©Authors, 2026, College of Science, University of Mosul.

Introduction

Geomorphometry is the measurement and mathematical study of the Earth's surface configuration, including the dimensions and shape of its landforms (Minár et al., 2024). The geomorphometric analysis is accomplished by measuring the linear, aerial, relief, and gradient of the channel network and the contributing ground slope of the basin (Garzon et al., 2023). An area's drainage lines help describe the evolution of the region's geomorphometry and explain its current three-dimensional geometry. Shape indices, a vital component of a

watershed's characteristics, are used in drainage basin geomorphometry to quantify basin shape and describe the hydrological features of a river basin (Zhou et al., 2023). The drainage basin analysis is crucial in any hydrological investigation, including pedology, environmental assessment, groundwater management, and groundwater potential assessment. According to hydrologists and geomorphologists, the relationship between runoff characteristics and drainage basin systems' geographic and geomorphic features is nearly significant. The physiographic characteristics of drainage basins, such as size, shape, slope, drainage density, and stream lengths, are associated with numerous significant hydrological phenomena (Pinto et al., 2023).

Therefore, water resources must be evaluated for the economy and the sustainability of livelihoods. Plans for development and management are also necessary if the ecosystem is to endure and keep supplying local communities with essential products and services. New methods of managing water and basins also require the best and most sustainable use of freshwater resources. Quantitative geomorphometry analysis of the watershed can provide the hydrological nature of the rocks within the watershed, which is essential information for watershed management plans (Iacobucci et al., 2024). A watershed's fundamental unit is its stream network, which shows its hydrological, geological, and structural configuration. For the management and execution of conservation measures, an understanding of the watershed's topography, stream network, and its pattern, and geological and geomorphological setup is necessary (Anya and Bhuiyan, 2024). Different regional hydrological models developed using the watershed's geomorphological features are used to solve various hydrological issues in ungauged watersheds. A geomorphometric characterization of the watershed is crucial for assessing its hydrological set-up in conjunction with its geology and geomorphology (Minár et al., 2024).

The basic units for managing land and water resources are drainage basins, catchments, and sub-catchments (Newman et al., 2022). Morphometric analysis is crucial for hydrological research, drainage basin development, and drainage basin management (Lindsay et al., 2004). The two main factors influencing running water ecosystems operating at the basin scale are morphometric parameters and climate. River basin assessment, watershed prioritization for soil and water conservation, and watershed-level natural resource management greatly benefit from the quantitative analysis of morphometric parameters (Ahmad et al., 2024).

The study aims to determine the typical engineering features of the Hasab drainage basin, one of the seasonal river basins in the southern Iraqi desert. Some attributes include stream order, lengths, mean stream length, bifurcation rate, stream frequency, and river drainage patterns. The study suggests connections between the shape and size features of the Hasab Valley drainage network and the landforms and processes in the area. The study seeks to identify the key shape features of the Hasab Valley drainage network and examine the natural factors that influence it, as well as the area's water flow and landform patterns.

Materials and Methods

Study Site

The Hasab watershed (HWS) is located in the western part of the southern Iraqi desert within the administrative borders of the Al-Najaf Governorate (Al-Abadi et al., 2015). It is bordered to the north by the south and southeastern parts of the Al-Najaf Sea and the Al-Tok Marsh. In contrast, to the south, it is bordered by the Jal Abu Khuwayma area near the Iraqi-Saudi border (Fig. 1). The HWS extends between latitudes (30°48′12″N – 31°49′18.331″N) north and longitudes (43°09′3.559″E – 44°22′30.496″E) east. It is one of the seasonal valleys in the southern Iraqi desert within the regions of the lower valleys and the Al-Hejar area. The area of the HWS is 3718.362 km², with a perimeter of 468.274 km, and a total length of 150.801 km, starting from its upper sources near Dhahrat Hasab and Jal Abu Khuwayma and

ending at its mouth near Al-Tok Marsh. The HWS is characterized by a relatively low-altitude plateau (Fig. 4) and its gradual slope from the southwest towards the northeast (Fig. 1).

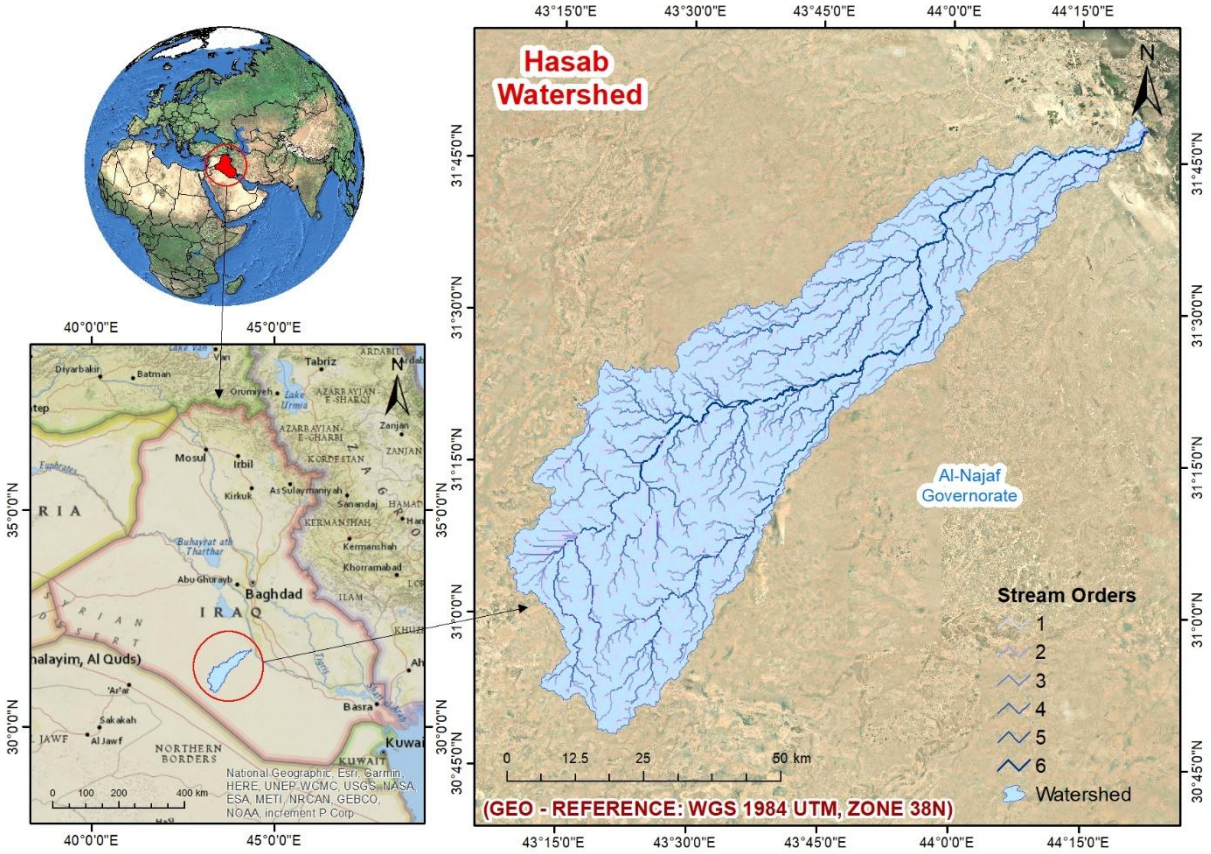

Fig. 1. Location of the Hasab watershed in Iraq.

The general slope rate is 2.466 m/km, and the varying elevations between its parts characterize the basin. The highest elevation in its upper sources in its southwestern part reached 390 m above sea level (Figs. 2 – 4). The lowest elevation reached 20 m (a.s.l) in the estuary area near Al-Tok Marsh and Bahr Al-Najaf. The HWS is characterized by increased ruggedness in its upper parts, representing the source area extending between the contour lines 390 - 280 m (a.s.l). This area represents the youth stage according to the phases of the Davisian cycle of the development stages of river basins, where many topographic features are spread, represented by plateaus, hills, fault edges, and other topographic features (Maaroof et al., 2025). The central area of HWS, which represents the maturity stage of the Davisian geomorphological cycle, is located between contour lines 280-130 m (a.s.l). It represents all the landforms in the southern Iraqi desert (Maaroof, 2022). It is less steep and rugged than the first region. Its level decreases gradually until it reaches the estuary region, which represents the aging stage of the geomorphological cycle and is located between contour lines (130 – 20) m (a.s.l).

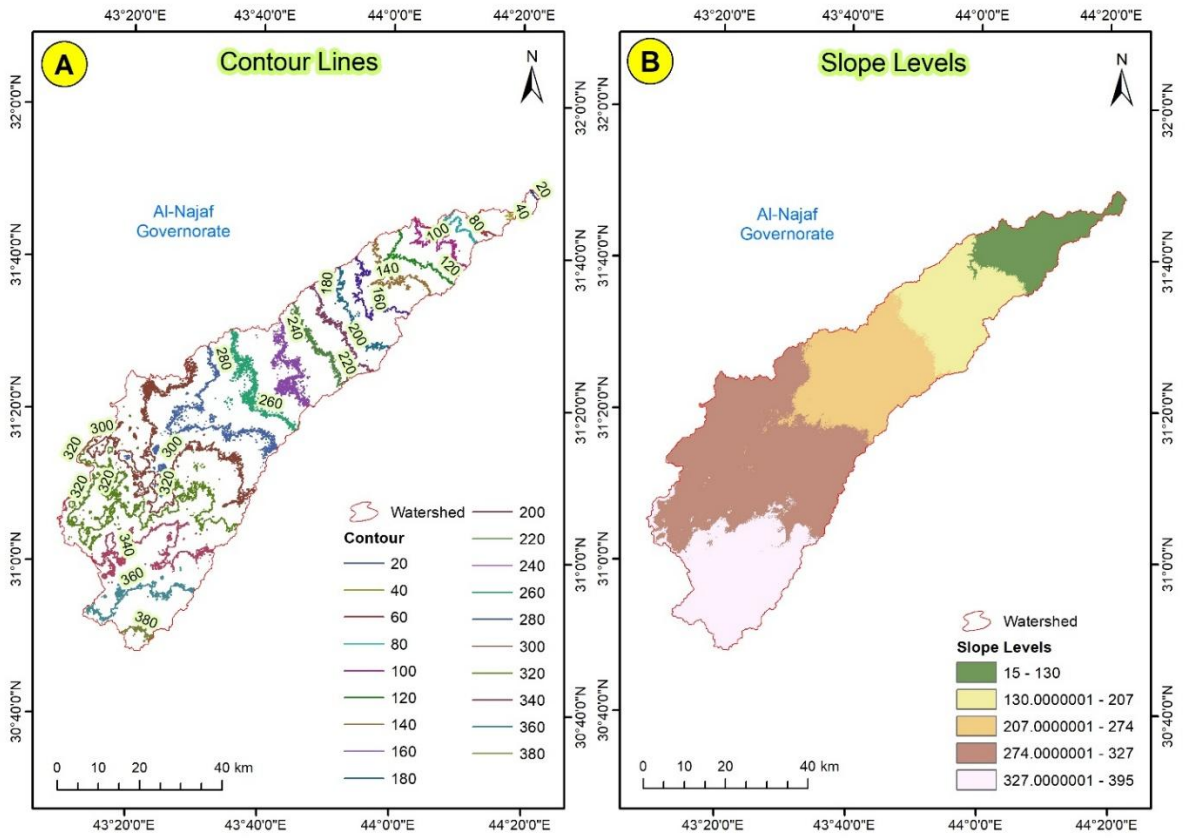

Fig. 2. (A) Contour lines and (B) Slope Levels of the Hasab watershed.

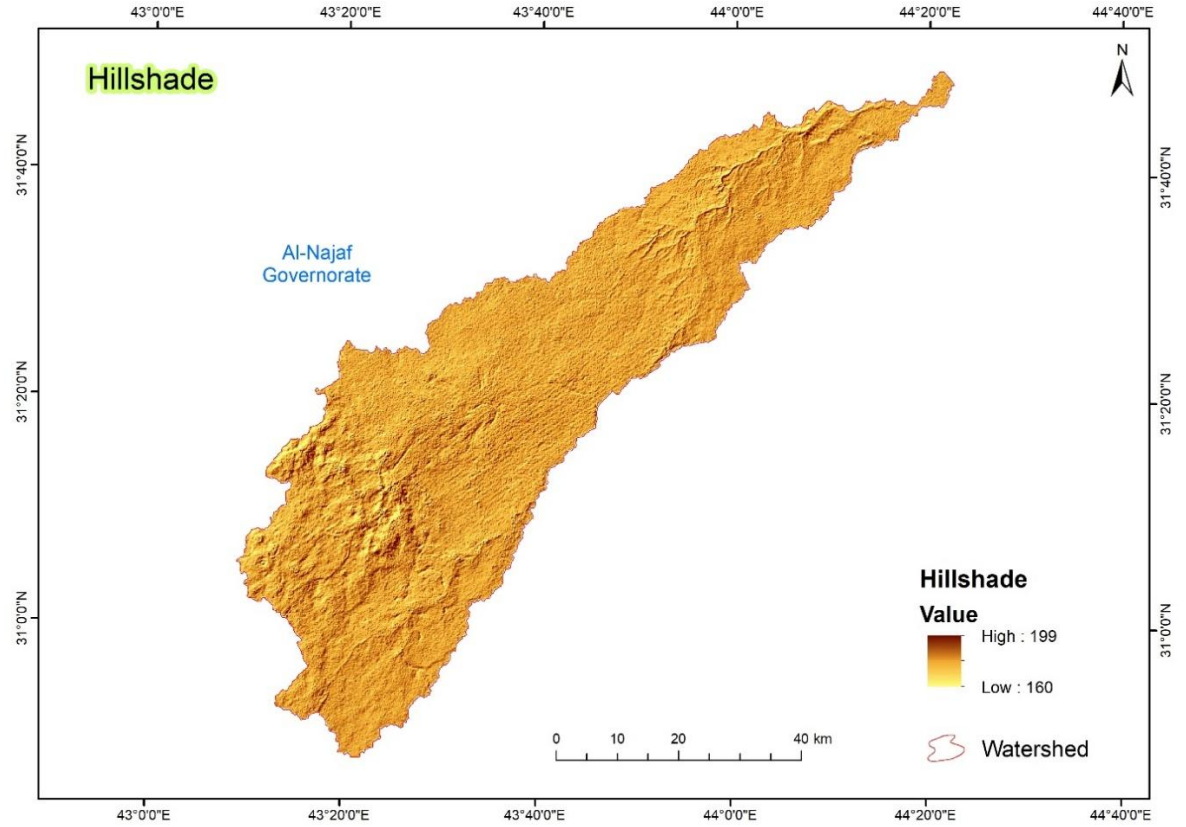

Fig. 3. The Hillshade of the Hasab watershed.

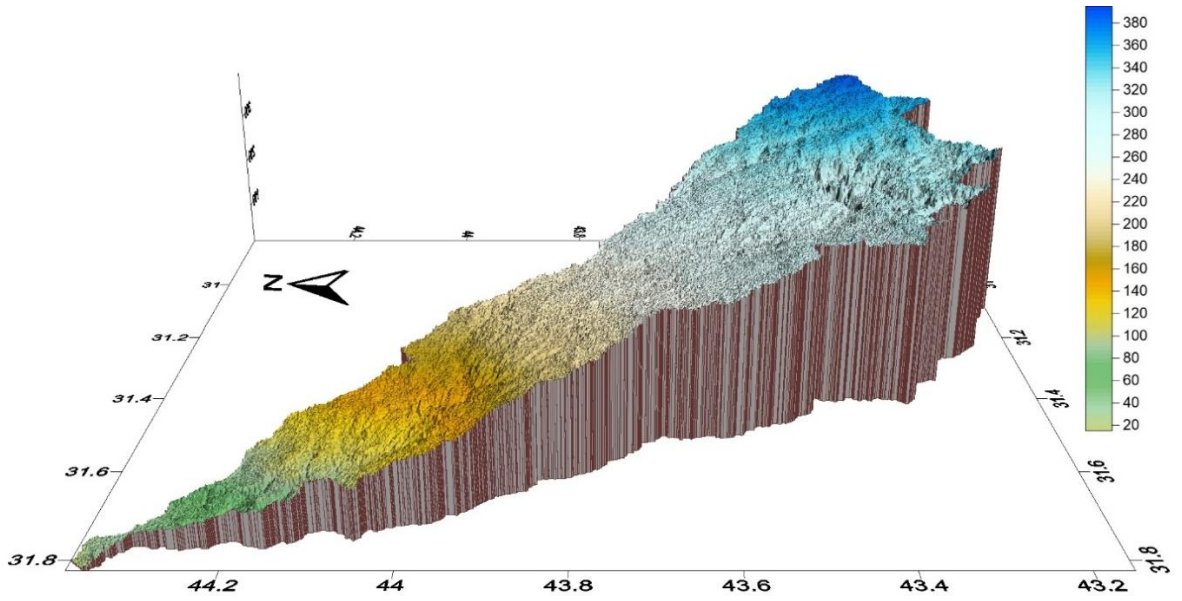

Fig. 4. The 3D model of the Hasab watershed.

Geologically, the study area consists of geological formations that vary according to their sedimentary environment (Maaroof et al., 2021). Some were deposited under continental environments, resulting from marine regression, while others were deposited under marine environments, resulting from marine transgression (Sissakian and Fouad, 2015). The ages of these formations ranged from the Upper Eocene to the Holocene. The causes of marine regression and submergence are due to the tectonic activity upon the exposed region it was exposed to during its geological history, resulting in changes in sea level and climate (Al-Jibouri and Gayara, 2015). The Fat'ha Formation is exposed in the northern parts of the study area. It contains basal breccia and sandstone with a thickness of 3 – 6 m and occupies an area of 37.46 km², representing 1.007% of the total area. The Ghar Formation is exposed in the northern parts of the study area and consists of red mudstone, fine sandstone, and gravelly sandstone with layers of chalky sandstone and basal breccia; it occupies an area of 179.75 km2, representing 4.83% (Table 1) (Ma'ala, 2009). The Dammam Formation is one of the most significant geological formations in the study area (Fig. 4), and it may have been formed during the Eocene (Al-Jiburi and Al-Basrawi, 2009). It was divided into two members (middle and lower) based on lithologic, physical, and fossil changes. The first is the Middle Dammam Formation, which is exposed across the northern and central parts of the study area (Fig. 4) with an area of 1563.464 km², representing 42.04% (Table 1). The Lower Dammam Formation is exposed across the southern parts of the study area, with an area of 1452 km^2, representing 39.04 % (Jassim and Al-Jiburi, 2009).

Table 1: Geological formations, their areas, and percentages in the study area.

Formation	Period	Area (km^2)	Percentage (%)
Depression fills deposits	Quaternary	97.604	2.624
Fatha Formation	Miocene	37.46	1.007
Gypcrete deposits	Quaternary	21.65	0.582
Ghar Formation	Miocene	179.75	4.834
Lower Dammam Formation-Jill	Eocene	1452	39.049
Middle Dammam Formation	Eocene	1563.464	42.047
Umm Er Radhuma – Akashat	Paleocene	240.999	6.481
Lower Zahra Formation	Pleistocene	60.19	1.618
Upper Zahra Formation	Pleistocene	65.23	1.754

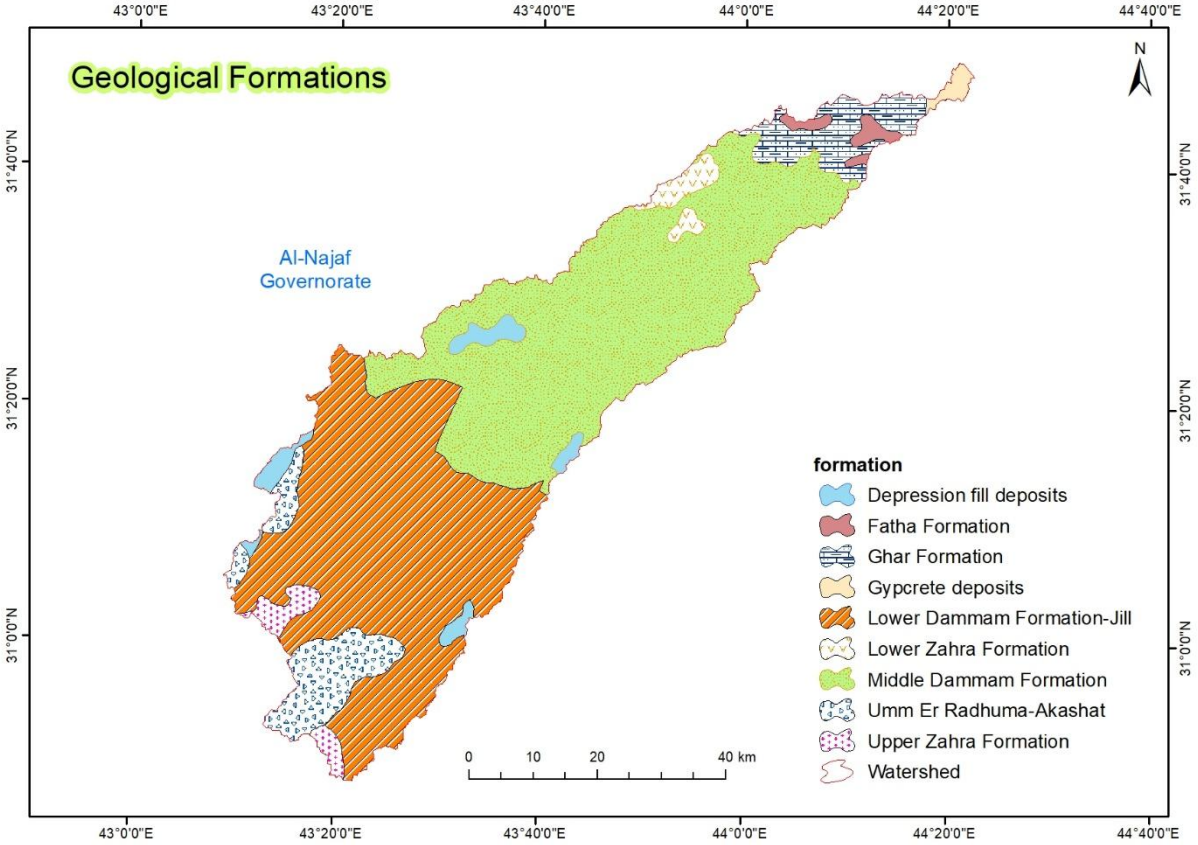

Fig. 5. Geological formations of the Hasab watershed.

Climatically, there is an apparent seasonal variation in temperature rates (Al-Hasani et al., 2024a). The temperature increases in the summer months (June, July, and August), reaching its highest in July at 37.3 °C (Fig. 6). In winter, the temperature is relatively moderate (Al-Hasani et al., 2024b). The temperature tends to decrease, with the lowest recorded in January at 10.9 °C. Rainfall is variable and fluctuating, characterized by its seasonality (AL- Hasani et al., 2025c). It falls at relatively spaced intervals as showers that quickly turn into torrential floods, eroding the earth's surface and forming its slopes (Maaroof et al., 2023). The highest rainfall value was recorded in December at 16.3 mm, while the lowest was recorded in May and October at 4.6 mm each (Şarlak and Mahmood Agha, 2018). The northern and northwestern winds dominate the study area and are similar to the winds over Iraq's central and southern regions, with an annual average of 2.6 m/s. Wind speed increases in the summer months (June, July, August), reaching 3.2, 4.1, and 2.9 m/s, respectively, and decreases in the winter months (November, December, January), reaching 1.8, 1.4, and 2.1 m/s, respectively.

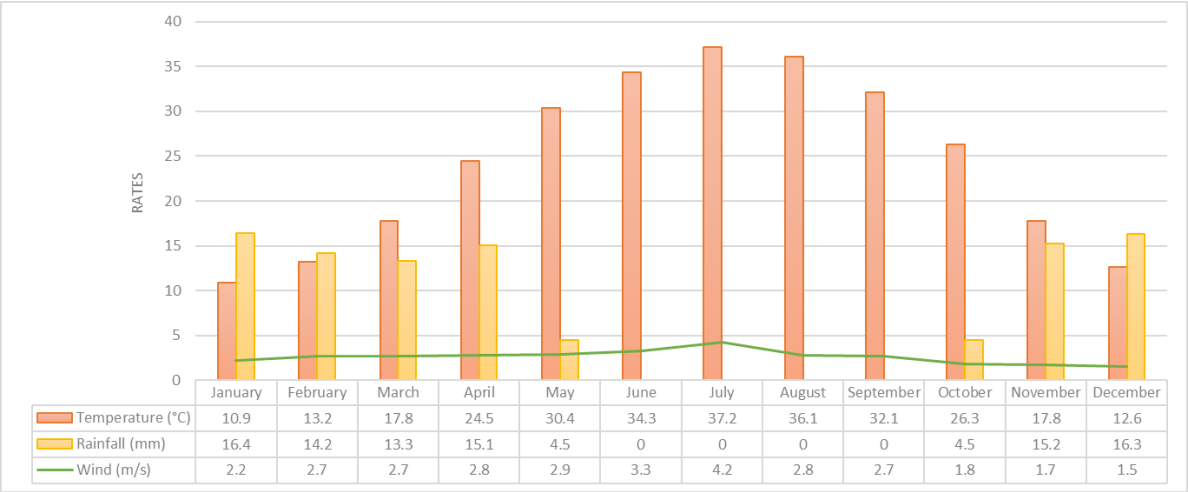

Fig. 6. Temperature, precipitation, and wind speed data for the study area from 1990 to 2020 from the Al-Najaf Climatic Station. Iraq | World Meteorological Organization (wmo. int)

The Hasab watershed is divided into four sub-watersheds:

1. Hasab sub-watershed (1) (HSW1): This sub-watershed is located in the eastern part of the study area. It has an area of 1600.53 km², a perimeter of 433.866 km, and a length of 121.422 km (Table 2 and Figs 7 and 8).

2. Hasab sub-watershed (2) (HSW2): This sub-watershed is located in the western part of the study area. It has an area of 517.364 km2, a perimeter of 143.776 km, and a length of 47.183 km (Table 2 and Figs 7 and 8).

3. Hasab sub-watershed (3) (HSW3): This sub-watershed is located in the southern part of the study area. It has an area of 725.85 km², a perimeter of 230.457 km, and a length of 230.457 km (Table 2 and Figs 7 and 8).

4. Hasab sub-watershed (4) (HSW4): This sub-watershed is located in the southern part of the study area. It has an area of 874.699 km², a perimeter of 225 km, and a length of 59.762 km (Table 2 and Figs 7 and 8).

Table 2: Area, perimeter, and length of Hasab sub-watersheds.

Sub-watersheds	Area (km2)	Perimeter (km)	Length (km)
Hasab sub-watershed (1) (HSW1)	1600.53	433.866	121.422
Hasab sub-watershed (2) (HSW2)	517.364	143.776	47.183
Hasab sub-watershed (3) (HSW3)	725.85	230.457	81.636
Hasab sub-watershed (4) (HSW4)	874.699	225	59.762

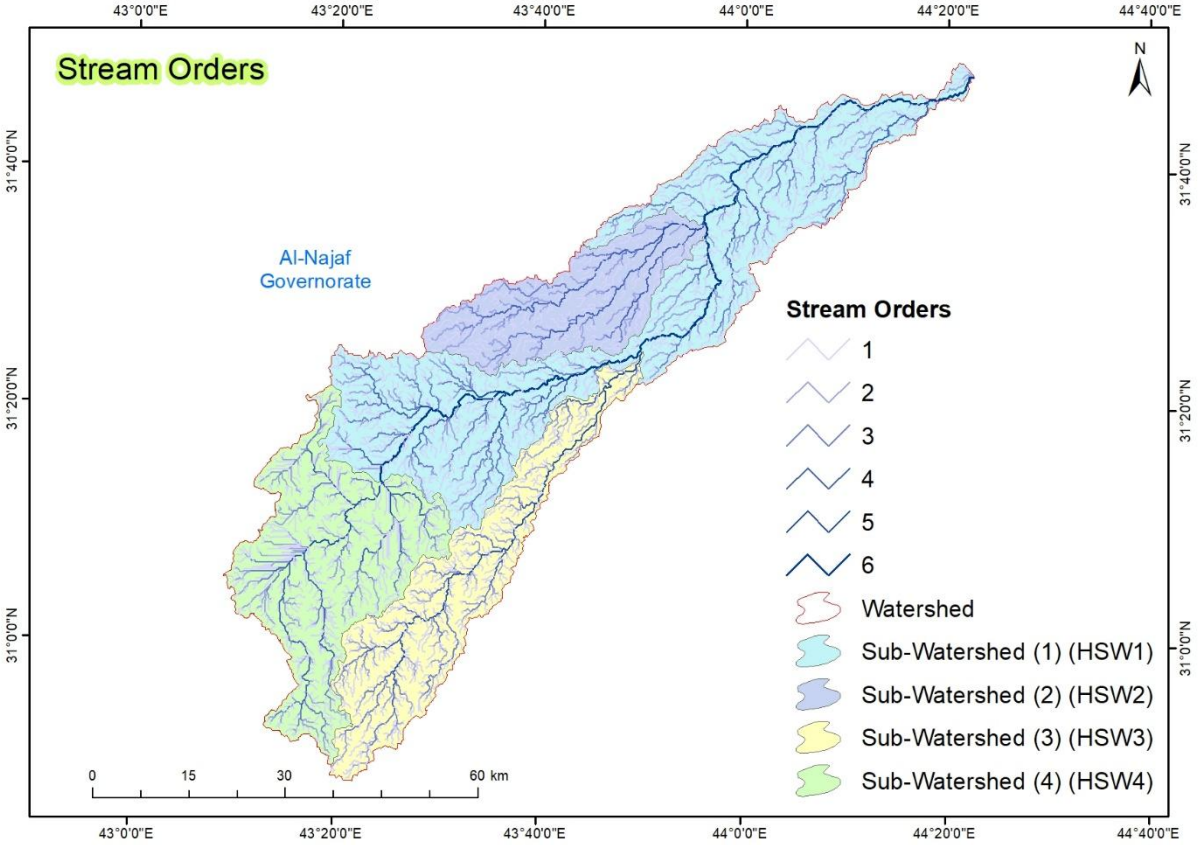

Fig. 7. Drainage basin network of the Hasab watershed and its sub-watersheds.

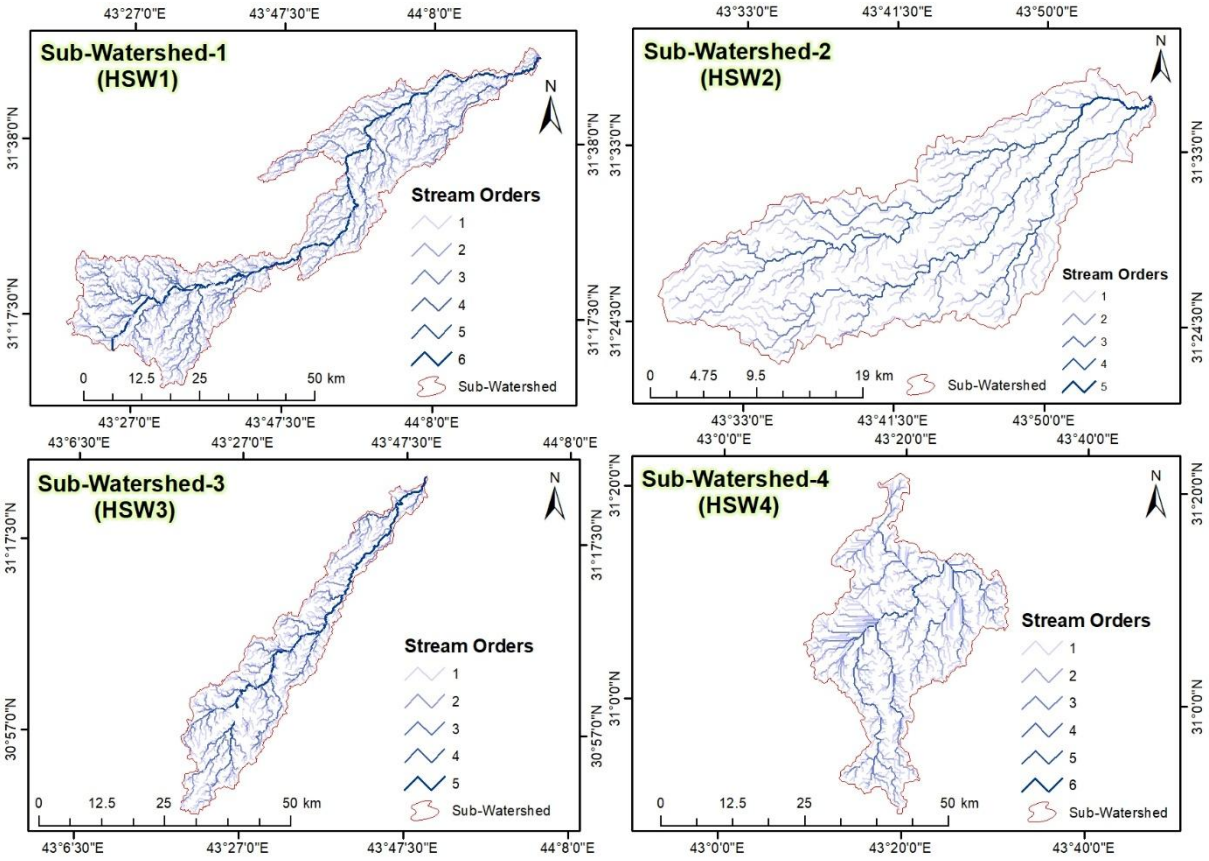

Fig. 8. Drainage basin network of Hasab Sub-watersheds.

Hydrologically, HWS is a seasonal watershed characterized by being a semi-arid area, and water does not flow in it except after being exposed to rainstorms that feed it with water (Ilaibi and Al-Sudani, 2019). Rain begins to fall from October until May, and water flows if the rainstorm continues and covers all parts of the area (Maaroof, 2024). The annual water flow volume in the basin can be determined by applying the Berkeley equation, which is based on the climate and topography elements (Maaroof, 2022b). Using the above equation, the results indicated that a watershed's expected annual flow volume is 0.001 billion/m3 (Table 3). The results were based on the amount of rainfall, the valley's area, the channel's average width, and the slope rate (Maaroof and Kareem, 2020). The equation's results were proportional; as the values of these variables increase, the flow rate increases, and vice versa.

Table 3: Expected annual runoff volume of the Hasab watershed.

Parameters	Units	Values
Area	(km^2)	3718.36
Length	(km)	150.80
Width	(km)	28.18
Annual rainfall	(mm)	8.3
Slope rate	(m/km)	2.45
Annual rainfall volume	(billion/m^3)	0.03
Width / Length	(km)	0.18
Expected annual flow	(billion/m^3)	0.001

Data Sources and Processing

An analysis and interpretation of the geomorphometric characteristics of the watershed was conducted utilizing the parameters presented in Table 4. The US Department of Defense provided the geospatial data through the Digital Elevation Model (DEM) (SRTM). Satellite imagery with a spatial resolution of 15 m was used from the US Landsat ETM+8 satellite for 2022. Additionally, the 1:100,000 topographic maps from the General Authority for Survey of Iraq and the 1:250,000 geological and hydrological maps from the Iraqi Geological Survey were used. By applying ArcGIS V.10.8, these data were incorporated into a topological model as raster layers (Maaroof, 2025). In addition to extracting the river drainage network at all levels, the main watershed and sub-watersheds were located and extracted as vector layers (Arosio et al., 2024). Additional software tools for spatial analysis, including Google Earth Pro V.7.1, ArcGIS Earth V.2, Surfer V.10, and Global Mapper V.11, were also utilized. Using a set of geomorphometric parameters, the stage of interpretation and geomorphometric analysis of the features of the river drainage network was advanced following the availability of an integrated geospatial database for the study area (Prasannakumar et al., 2011). Connecting and evaluating the factor, geomorphological process, and stage on the one hand, and forming the drainage network characteristics for a watershed on the other, was accomplished within the framework of geomorphological analysis (Maaroof and Kareem, 2023). Cartographic techniques also clarified the spatial dimensions of the watershed's geomorphometric features (Fig. 4).

Table 4: Geomorphometric parameters of the river drainage network.

Parameters	Symbol	Formula	Description	Reference
Stream orders	*(U)*	Hierarchical Rank	--	(Strahler, 1957)
Stream length	*(L_u)*	Length of the streams	--	(Schumm, 1956)
Mean stream length	*(L_{sm})*	$L_{sm} = L_u / N_u$	L_u = Total length of stream order (U) (km) N_u = Total number of stream orders (U) (km)	(Strahler, 1957)
Bifurcation ratio	*(R_b)*	$R_b = N_u / (N_u+1)$	N_u = Total number of stream orders (U) (km) $N_u + 1$ = Total Number of streams of its next order	(Horton, 1945)
Stream frequency	*(F_s)*	$F_s = N_u / A$	N_u = Total number of stream orders (U) (km) A = Area of the watershed (km^2)	(Horton, 1945)
Drainage density	*(D_d)*	$D_d = L_u / A$	L_u = Total length of stream order (U) (km) A = Area of the basin (km^2)	(Horton, 1945)
Basin texture	*(T)*	$T = N_u / P$	N_u = Total number of stream orders (U) (km) P = Perimeter (km)	(Smith, 1950)
Constant of channel maintenance	*(M_c)*	$M_c = 1/D_d$	D_d = Drainage density	(Schumm, 1956)

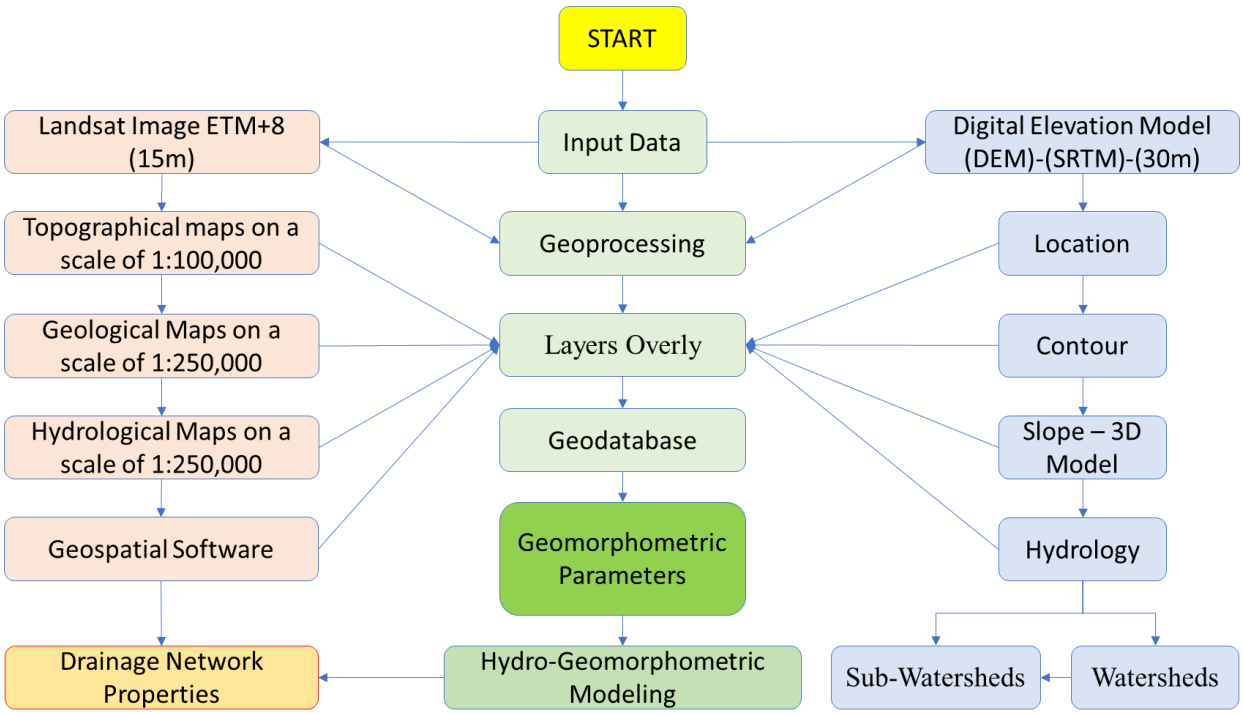

Fig. 9. Flowchart of methodology.

Results and Discussion

Stream orders (U)

The stream orders in the study area are classified according to the method presented by Strahler (1957). According to this method, the watercourses of small streams and torrents that do not meet any tributary from their upper reaches are classified as first-order tributaries. When two first-order streams meet, a second-order stream is formed; when two second-order streams meet, a third-order stream is formed, and so on for the remaining orders. To simplify, a new higher order is formed when the two lower orders meet. The total number of river orders in the Hasab watershed was 6 (Figs. 7 and 8) and Table 4. Their numbers varied from one order to another, according to Horton's law for waterways (Arefin et al., 2020). This confirms that waterways in their orders follow a geometric progression, with the highest limit being the first order, and then they begin to decrease as river orders increase (Mahala, 2020). The first order was 2677, with a percentage of 35.316%, while the second was 1762, with a rate of 23.245%. The third order was 1258, with a percentage of 16.596%; the fourth was 889, with a percentage of 11.728%; and the fifth order was 827, with a percentage of 10.910%. As for the sixth order, it was 167, with a percentage of 2.203%.

There is an apparent variation in the number of stream orders from one basin to another, which is normal, according to Strahler's explanation above (Strahler, 1957). In addition to the direct proportion to the basin area, the larger the area, the greater the number of valleys in the stream orders. Also, the difference in the hardness of the rock formations plays a significant role in the variation of river beds. Rugged rocks resist erosion processes, unlike less complicated stones exposed to these processes, and thus form more beds. In addition to the structural features of the faults and fractures that affect the area through which the streams run. The intensity of rainfall, slopes, the shape of the basin, and the density of vegetation all affect the diversity of stream orders.

Table 5: Stream orders of the Hasab watershed and its sub-watersheds.

Sub-watersheds	Number of stream orders						Total number
	First order	Second order	Third order	Fourth order	Fifth order	Sixth order	
Hasab sub-watershed (1) (HSW1)	1134	502	306	124	15	166	2247
Hasab sub-watershed (2) (HSW2)	327	146	70	93	12	--	648
Hasab sub-watershed (3) (HSW3)	532	502	378	160	525	--	2097
Hasab sub-watershed (4) (HSW4)	684	612	504	512	275	1	2588
The Total	2677	1762	1258	889	827	167	7580
Percentage %	35.316	23.245	16.596	11.728	10.910	2.203	100

Stream length (L_u)

The total stream lengths of the Hasab watershed were 4342.563 km (Table 6). Most of the lengths were located in large watersheds. Hasab sub-watershed (1) (HSW1) accounted for 50.882%, with a total of 2209.585 km. The Hasab sub-watershed (4) (HSW4) occupied the second place, with a percentage of 28.045% and a total length of 1217.902 km. The remaining sub-watersheds represented by Hasab sub-watersheds (2) and (3) were 9.100% and 11.971%, respectively, with a total length of 395.188 km and 519.888 km. At the level of river orders, the total length of the first order reached 2726.788 km, representing 39.554% of the total length of the channels. Meanwhile, the length of the second-order channels reached 1195.247 km, representing 17.338%. As for the remaining orders (third, fourth, fifth, and sixth), their lengths reached 614.265 km, 334.133 km, 137.578 km, and 1885.653 km, respectively, with percentages of 8.910%, 4.846%, 1.995%, and 27.353%.

Table 6: Stream length of the Hasab watershed and its sub-watersheds.

Sub-watersheds	Length of the stream (km)						Total length (km)	%
	First order	Second order	Third order	Fourth order	Fifth order	Sixth order		
Hasab sub-watershed (1) (HSW1)	1105.740	518.718	303.842	114.482	14.243	152.558	2209.585	50.882
Hasab sub-watershed (2) (HSW2)	395.188	171.258	71.635	94.904	9.519	742.507	395.188	9.100
Hasab sub-watershed (3) (HSW3)	519.888	241.693	112.917	34.040	82.046	990.587	519.888	11.971
Hasab sub-watershed (4) (HSW4)	705.972	263.578	125.871	90.707	31.770	0.001	1217.902	28.045
The Total	2726.788	1195.247	614.265	334.133	137.578	1885.653	4342.563	100
Percentage %	39.554	17.338	8.910	4.846	1.995	27.353	100	100

Mean stream length (L_{sm})

According to Horton (1945), there is a direct correlation between the length of the river channel and its order; as the order of the channel increases, the average length increases by three times. In specific streams, the ratio of the lengths of these channels varies due to natural factors and conditions along the stream. Adjusting Horton's law of waterway lengths (Strahler, 1957a) verified that the channel length increases in a constant ratio from one order to another, three times the minor order. Additionally, Strahler (1957) proposed that the average lengths of waterways in successive orders tend to add up to a geometric progression, starting with the first-order average length and increasing by a fixed length ratio.

The average length of an order increases according to a geometric progression, which is consistent with what Horton and Strehler mentioned above. Smaller average stream lengths characterize the lower orders, while larger average stream lengths characterize the higher orders. The average of the first order was 1.048 km, followed by the second order with 0.503 km, while the average of the third order was 0.304 km, and the fourth order was 0.218 km, while the fifth and sixth orders were 0.154 and 1.207 km, respectively. As for the sub-watersheds, the variation is apparent in the average stream length, with the Hasab sub-watershed (1) (HSW1) reaching a value of 2.397 km, representing 36.389%, the highest percentage. The Hasab sub-watershed (4) (HSW4) came in second place with a value of 2.005 km with a percentage of 30.438. The reason for the variation in the length rates of waterways in the study area is attributed to several reasons represented by the diversity in geological formations, which in turn was reflected in the rock diversity in the region, which ranged between hard rocks that are resistant to geomorphological processes and others that are less

hard and have weak resistance to these processes, in addition to the apparent diversity in slope rates and the tremendous and distinct role of these slopes in increasing the speed of running water and thus increasing erosion rates, in addition to the effect of the structural composition represented by cracks, fractures, and joints.

Table 7: Average length of streams for the Hasab watershed and its sub-watersheds.

Sub-watersheds	Average length of streams according to their orders (km)						Average (km)	%
	First order	Second order	Third order	Fourth order	Fifth order	Sixth order		
Hasab sub-watershed (1) (HSW1)	0.975	0.516	0.330	0.230	0.189	0.153	2.397	36.389
Hasab sub-watershed (2) (HSW2)	1.208	0.586	0.341	0.255	0.158	2.549	1.208	18.339
Hasab sub-watershed (3) (HSW3)	0.977	0.481	0.298	0.212	0.156	2.126	0.977	14.832
Hasab sub-watershed (4) (HSW4)	1.032	0.430	0.249	0.177	0.115	0.0002	2.005	30.438
Average	1.048	0.503	0.304	0.218	0.154	1.207	6.587	100
Percentage %	30.502	14.647	8.862	6.359	4.496	35.131	100	100

Bifurcation ratio (R_b)

As proposed by Horton (1945), it is the ratio of the number of streams of one order to the number of streams of the following order. It is calculated by finding the average bifurcation within the basin as a whole. This parameter completes the relationship between river order and stream numbers. (Strahler, 1957a) reported that the average bifurcation ratio is 3.5 for each order and the order above it, meaning that first-order streams are three and a half times larger than second-order streams, and second-order streams are also three and a half times larger than third-order streams, forming an inverse geometric relationship (Strahler, 1954). The bifurcation ratio of the sub-watersheds shows that three-quarters of the first-order streams develop into second-order streams through river capture processes. The first-order streams are more significant in number, length, and bifurcation ratio than the other orders. This indicates a need for a better proportion between the lengths and numbers of lower-order streams and the main streams due to the significant changes these streams experience from water erosion (Niculiță, 2020). This process does not stop at this point; however, it continues transforming second-order streams into third-order streams in a geometric progression expressed by the bifurcation ratio according to Horton's law for the number of streams. The bifurcation ratios of sub-watersheds vary from one sub-watershed to another, according to the geological and climatic data prevailing in the region. The bifurcation ratio of the Hasab sub-watershed (4) (HSW4) is recorded as 10.235, the highest among all sub-watersheds (Table 8). The remaining sub-watersheds varied in their ratios, reaching 2.151, 2.318, and 1.263 for the sub-watersheds (HSW1), (HSW2), and (HSW3), respectively.

Table 8: Bifurcation ratio of the Hasab watershed and its sub-watersheds.

Watersheds	Orders	Number of streams	Bifurcation ratio	Average
Hasab sub-watershed (1) (HSW1)	1	1133	1.128	2.151
	2	1004	1.093	
	3	918	1.850	
	4	496	6.613	
	5	75	0.075	
	6	996	-	
Hasab sub-watershed (2) (HSW2)	1	327	1.119	2.318
	2	292	1.390	
	3	210	0.564	
	4	372	6.2	
	5	60	-	
Hasab sub-watershed (3) (HSW3)	1	532	1.059	1.263
	2	502	1.328	
	3	378	2.362	
	4	160	0.304	
	5	525	-	
Hasab sub-watershed (4) (HSW4)	1	684	1.117	10.235
	2	612	1.214	
	3	504	0.984	
	4	512	1.861	
	5	275	46	
	6	6	-	

Stream frequency (F_s)

This parameter indicates the frequency of streams within drainage basins and quantifies the ratio of drainage channels to basin area. The stream frequency rate suggests the density of watercourses per km² and the dissection in the drainage basin's configuration (Vörös et al., 2022). The rise in the average length of streams correlates with the increase in streams featuring a gentle slope. This can be utilized to discern various hydrological and geomorphological attributes. It illustrates the density of watercourses per square kilometer and their contribution to the severity of basin fragmentation, which escalates with the frequency of rivers per square kilometer (Rai et al., 2018).

The stream frequency of the Hasab watershed was 1.421 km/km2 (Table 9), and the sub-watershed rate increased to 2.126 km/km2. The sub-watersheds varied in their values, with Hasab sub-watershed (4) (HSW4) reaching 2.958 km/km2, the highest value, and Hasab sub-watershed (2) (HSW2) reaching 1.252 km/km2, the lowest value. The variation in the river frequency values of the Hasab watershed is related to the local differences in the geological structure and topography of the basin, which control the number of tributaries and streams. In addition to the effect of the spatial characteristics of the sub-watersheds, the large area of sub-watersheds was characterized by low river frequency values, as in the Hasab sub-watershed (1 and 2). While the river frequency values increased in the small area of sub-watersheds, as in the Hasab sub-watershed (3 and 2). Also, adequate rainfall plays a significant role in increasing river frequency, which rises with the slope and prevalence of hard rocks in the basin.

Table 9: Stream frequency, drainage density, basin texture, and constant channel maintenance of the Hasab watershed and its sub-watersheds.

Watersheds	Stream frequency (km/km^2)	Drainage density (km/km^2)	Basin texture (Stream/km)	The constant of channel maintenance (km^2/km)
Hasab watershed	1.421	1.387	11.290	0.720
Hasab sub-watershed (1) (HSW1)	1.403	1.380	5.179	0.724
Hasab sub-watershed (2) (HSW2)	1.252	0.763	4.507	1.309
Hasab sub-watershed (3) (HSW3)	2.889	0.716	9.099	1.396
Hasab sub-watershed (4) (HSW4)	2.958	1.392	11.502	0.718
Average	2.126	1.063	7.571	1.036

Drainage density (D_d)

The results of this parameter reflect climatic conditions, especially rainfall and its quantity, geological characteristics, rock type, permeability, surface and slope, and vegetation density (Resmi, et al., 2019). The drainage density of the Hasab watershed was 1.387 km/km2 (Table 9), indicating that every 1 square kilometer of the catchment area has 1.387 square kilometers of stream to drain water. The average drainage density of sub-watersheds was 1.063 km/km2. The rest of the sub-watersheds varied from the above average, with the Hasab sub-watershed (4) (HSW4) having the highest value at 1.392 km/km². At the same time, it was 0.716 km/km2 for the Hasab sub-watershed (3) (HSW3), which is the lowest value. The low drainage density results from the large basin areas and their location in regions severely affected by erosion and chemical weathering, where Quaternary sediments and dolomite rocks are exposed. In addition to the late erosion stage that the basin is experiencing, characterized by a low slope, the upper levels are dominant due to their relative length and small numbers.

The basins with high drainage density are mainly due to the hardness of their limestone rocks and high clay content, which reduces permeability and increases surface runoff volume at the expense of filtration rate. In addition to the increased slope in these areas, which affected the increase in the numbers of the first order, there was an increase in their lengths at the expense of the rest of the other orders. Partially, the second order also plays a role in this increase, as the abundance of faults contributed to this increase in their lengths at the expense of the other orders. The second-order valleys experience more vertical and retrograde erosion

than lateral erosion because the dry conditions do not allow for the rapid growth of these channels, which acquired most of their characteristics in the Pleistocene era.

Basin texture (T)

It is an indicator to measure the degree of basin discontinuity by river channels. This parameter is affected by several factors, such as climate, geological structure, natural vegetation, and the geomorphological stage through which the valley passes (Fenta et al., 2017). Strahler (1957) found the relationship between the Basin texture rate and the Drainage density. He concluded that basins composed of solid sandstone rocks are characterized by low drainage density values and basin texture rates, as the streams are spaced apart. The Basin texture rate for the Hasab watershed was 11.290 Stream/km (Table 9), an average value according to the scale developed by Morisawa in 1989 (Table 10). The sub-watershed remained static in its values, reaching 11.502 Stream/km for the Hasab sub-watershed (4) (HSW4), which is the highest value. At the same time, it reached 4.507 Stream/km for the Hasab sub-watershed (2) (HSW2), which is the lowest value.

Most of the basins in the study area fall within the medium texture level because the weak rock components, such as sandstone and dolomite, resist water erosion processes. In addition, some of these valleys are located in the advanced stage of the erosion cycle, characterized by flatness. By studying the relationship between basin texture and drainage density, it becomes clear that they are directly proportional, meaning the topographic texture rate increases as drainage density increases. The valleys are characterized by low texture rate and low drainage density values for most of the tributary valleys. The geomorphological stage factor played a significant role in determining the locations of the drainage basins. Low drainage density and low topographic texture rate values characterized small basins that have made little progress in the geomorphological stage. The large valleys that have made good progress in the geomorphological stage, such as the Hasab sub-watershed (4), were characterized by high drainage density values and high topographic texture rate.

Table 10: Classification of watersheds based on topographic texture patterns according to (Morisawa, 1989).

Category	Type	Rate (Stream/km)	Description
1	Coarse	Less than 8	High-permeability rocks with abundant vegetation.
2	medium	8 - 20	High-permeability rocks with abundant vegetation and rainfall.
3	fine	20 - 200	Low-permeability rocks with large amounts of rainfall and little vegetation.
4	very fine	More than 200	Low-permeability rocks with little vegetation and moderate amounts of rainfall.

The constant of channel maintenance (M_c)

This parameter was proposed by (Schumm, 1956) Moreover, indicates the area needed to supply the river network with water. Increasing the value of this parameter indicates that the basin area is larger at the expense of the length of its channels. The constant channel maintenance for the Hasab watershed was 0.720 km2/km (Table 9), which means that every kilometer of stream length is fed by an area estimated at 0.720 km2. The values of this parameter varied in the sub-watersheds, where it was 1.396 km2/km for Hasab sub-watershed (3) (HSW3), which is the highest value, and 0.718 km2/km for Hasab sub-watershed (4) (HSW4), which is the lowest value. The above values indicate that the constant of channel maintenance values is close, which suggests the similarity of the climatic conditions that affected the formation of the river networks of the watersheds of the study area, together with the effect of the geological structure conditions that the area experienced. The decrease in the values of this parameter in some sub-watersheds is due to the increase in stream lengths at the expense of the basin area.

Conclusion

Stream order diversity varies across basins and is influenced by factors like basin area, rock formation hardness, structural features, rainfall intensity, slopes, basin shape, and

vegetation density. The length rates of the watercourse in the study area vary due to geological diversity, rock diversity, slope rates, and structural composition, with rugged rocks resisting processes and slopes increasing erosion. The bifurcation ratio of sub-watersheds reveals that first-order streams transition into second-order ones due to river captivity, indicating a need for increased water erosion proportion. The frequency of river values in the Hasab watershed varies based on local geological structure and topography. Large sub-watersheds have low frequencies, while small sub-watersheds experience increased frequencies due to rainfall and slope. The basins have low drainage density due to their large areas and surrounding settlements. This is further characterized by erosion and chemical weathering processes due to the hardness of limestone and the high clay content. Moreover, the high drainage density, reduced permeability, and increased surface runoff volume contribute to this. The first order has become longer, while the second has increased due to the abundance of faults. Second-order valleys experience more vertical and retrograde erosion than lateral erosion due to dry conditions. The basins of the study area are primarily intermediate, with some valleys in the advanced stages of erosion. Basin texture and drainage density are directly proportional, with geomorphological stages influencing basin locations. The constant channel maintenance values suggest similar climatic and geological conditions affecting river network formation in the study area. However, certain sub-watersheds experience decreased values due to increased stream lengths.

Acknowledgements

The authors would like to thank the Babylon Center for Civilization and Historical Studies at the University of Babylon, the Department of Geography at the University of Misan, Iraq, and the Department of Civil Engineering and Built Environment at Liverpool John Moores University for their scientific support throughout the study.

Conflict of Interest

The authors declare that there are no conflicts of interest regarding the publication of this manuscript.

Credit authorship contribution statement

Bashar F. Maaroof: Project administration, Conceptualization, Data curation, Formal analysis, Investigation, Methodology, Supervision, Validation, Visualization, Software, Writing – original draft. **Hashim H. Kareem:** Supervision, Visualization, Methodology, Resources, Validation, Writing – review and editing. **Jaffar H. Al-Zubaydi:** Supervise, data curation, formal analysis, methodology, software, writing – review and editing. **Rayan G. Thannoun:** Visualization, Data curation, Formal analysis, Methodology, Software, Writing – review and editing. **Manal Sh. Al-Kubaisi:** Formal analysis, Methodology, Validation. **Ban Al-Hasani:** Formal analysis, Methodology, Validation. **Mawada Abdellatif:** Formal analysis, Methodology, Validation. **Iacopo Carnacina:** Formal analysis, Methodology, Validation.

References

Ahmad, S., Shazil, M.S., Hassan, A.F., and Afzal, B., 2024. Geo-spatial assessment of geomorphic characteristics of Swat Valley, Pakistan. Results in Earth Sciences, 2, 100042. https://doi.org/10.1016/j.rines.2024.100042

AL-Hasani, B., Abdellatif, M., Carnacina, I., Harris, C., Maaroof, B.F., and Zubaidi, S.L., 2025c. Rainwater Harvesting Site Assessment Using Geospatial Technologies in a Semi-Arid Region: Toward Water Sustainability. *Water*, *17*(15), 2317. https://doi.org/10.3390/w17152317

Al-Abadi, A.M., Pradhan, B. and Shahid, S., 2015. Prediction of groundwater flowing well zone at An-Najif Province, central Iraq using evidential belief functions model and GIS. Environmental Monitoring and Assessment, 188(10). https://doi.org/10.1007/s10661-016-5564-0

Al-Hasani, B., Abdellatif, M., Carnacina, I., Harris, C., Al-Quraishi, A.M.F., and Maaroof, B. F., 2024b. Assessing Climate Change Impacts on Rainfall-Runoff in Northern Iraq: A Case Study of Kirkuk Governorate, a Semi-Arid Region. In Handbook of Environmental Chemistry (Vol. 136, pp. 93–111). Springer Science and Business Media Deutschland GmbH. https://doi.org/10.1007/698_2024_1154

Al-Hasani, B., Abdellatif, M., Carnacina, I., Harris, C., Al-Quraishi, A., Maaroof, B.F., and Zubaidi, S.L., 2024a. Integrated geospatial approach for adaptive rainwater harvesting site selection under the impact of climate change. Stochastic Environmental Research and Risk Assessment, 38(3), 1009–1033. https://doi.org/10.1007/s00477-023-02611-0

Al-Jibouri, B.S.M. and Gayara, A.D., 2015. PALEOCENE SEQUENCE DEVELOPMENT IN THE IRAQI WESTERN DESERT. In Iraqi Bulletin of Geology and Mining (Vol. 11, Issue 3).

Al-Jiburi, H.K. and Al-Basrawi, N.H., 2009. Hydrogeology of Iraqi Southern Desert. Iraqi Bulletin of Geology and Mining, 2, 77–91.

Anya, B. and Bhuiyan, C., 2024. Hydro-morphometry of a trans-Himalayan River basin: Spatial variance, inference and significance. Environmental Challenges, 15. https://doi.org/10.1016/j.envc.2024.100890

Arefin, R., Mohir, M.M.I., and Alam, J., 2020. Watershed prioritization for soil and water conservation aspect using GIS and remote sensing: PCA-based approach at northern elevated tract Bangladesh. Applied Water Science, 10(4). https://doi.org/10.1007/s13201-020-1176-5

Arosio, R., Gafeira, J., De Clippele, L.H., Wheeler, A.J., Huvenne, V.A.I., Sacchetti, F., Conti, L.A., and Lim, A., 2024. CoMMa: A GIS geomorphometry toolbox to map and measure confined landforms. Geomorphology, 458. https://doi.org/10.1016/j.geomorph.2024.109227

Fenta, A.A., Yasuda, H., Shimizu, K., Haregeweyn, N., and Woldearegay, K., 2017. Quantitative analysis and implications of drainage morphometry of the Agula watershed in the semi-arid northern Ethiopia. Applied Water Science, 7(7), 3825–3840. https://doi.org/10.1007/s13201-017-0534-4

Garzon, L.F.L., Johnson, M.F., Mount, N., and Gomez, H., 2023. Exploring the effects of catchment morphometry on overland flow response to extreme rainfall using a 2D hydraulic-hydrological model (IBER). Journal of Hydrology, 627. https://doi.org/10.1016/j.jhydrol.2023.130405

Horton, R.E., 1945. Erosional development of streams and their drainage basins; Hydrophysical approach to quantitative morphology. Bulletin of the Geological Society of America, 56(3), 275–370. https://doi.org/10.1130/0016-7606(1945)56[275:EDOSAT]2.0.CO;2

Iacobucci, G., Delchiaro, M., Troiani, F. and Nadali, D., 2024. Land-surface quantitative analysis for mapping and deciphering the construction processes of piedmont alluvial fans in the Anti-Lebanon Mountains. Geomorphology, 453. https://doi.org/10.1016/j.geomorph.2024.109148

Ilaibi, H. and Al-Sudani, Z., 2019. Estimation of Water Balance in Iraq using Meteorological Data. International Journal of Recent Engineering Science (IJRES), 6(5), 8–13. www.ijresonline.com8

Jassim, R.Z. and Al-Jiburi, B.S., 2009. Stratigraphy of Iraqi Southern Desert. Iraqi Bull. Geol. Min, Special Issue, 2009: Geology of Iraqi Southern Desert, pp. 53-76.

Lindsay, J.B., Creed, I.F., and Beall, F.D., 2004. Drainage basin morphometrics for depressional landscapes. Water Resources Research, 40(9). https://doi.org/10.1029/2004WR003322

Ma'ala, K.A., 2009. Geomorphology of Iraqi Southern Desert. Iraqi Bull. Geol. Min, Special Issue, 2009: Geology of Iraqi Southern Desert, p 77-91.

Maaroof, B.F., 2022a. Geomorphological Assessment Using Geoinformatics Applications of the Sloping System of Al-Ashaali Drainage Basin at Iraqi Southern Desert. Iraqi National Journal of Earth Science, 22(1), 38–54. https://doi.org/10.33899/earth.2022.133146.1009

Maaroof, B.F., 2022b. Geomorphometric Assessment of The River Drainage Network at Al-Shakak Basin (Iraq). Journal Of the Geographical Institute Jovan Cvijic Sasa, 72(1), 1–13. https://doi.org/10.2298/IJGI2201001M

Maaroof, B.F., 2024. Quantitative Analysis Using Geospatial Modeling of Al-Rahimawi Watershed's Shape Properties in The Iraqi Southern Desert. Bulletin Of the Iraq Natural History Museum, 18(2), 277–295. https://doi.org/10.26842/binhm.7.2024.18.2.0277

Maaroof, B.F., 2025. Fluvial Landforms Classification Using Geospatial Modeling of Al-Jazeera Eastern Region at Misan Governorate, Iraq. Iraqi National Journal of Earth Science, 25(2), 199–218. https://doi.org/10.33899/earth.2024.146564.1228

Maaroof, B.F., Al-Abdan, R.H. and Kareem, H.H., 2021. Geographical Assessment of Natural Resources at Abu-Hadair Drainage Basin in Al-Salman Desert. In Southern Iraq Indian Journal of Ecology (Vol. 48, Issue 3).

Maaroof, B.F. and Kareem, H.H., 2020. Water Erosion of the Slopes of Tayyar Drainage Basin in the Desert of Muthanna in Southern Iraq. In Indian Journal of Ecology (Vol. 47, Issue 3).

Maaroof, B.F. and Kareem, H.H., 2023. Geomorphological Analysis of Chemical Weathering Features in Al-Band Hills Area, Eastern of Misan Governorate, Iraq. Iraqi National Journal of Earth Science, 23(1), 67–84. https://doi.org/10.33899/earth.2023.137382.1034

Maaroof, B.F., Omran, M.H., Al-Qaim, F.F., Salman, J.M., Hussain, B.N., Abdellatif, M., Carnacina, I., Al-Hasani, B., Jawad, M.R., and Hussein, W.A., 2023. ENVIRONMENTAL ASSESSMENT OF AL-HILLAH RIVER POLLUTION AT BABIL GOVERNORATE (IRAQ). Journal of the Geographical Institute Jovan Cvijic SASA, 73(1), 1–16. https://doi.org/10.2298/IJGI2301001M

Maaroof, B., Kareem, H., Al-Zubaydi, J., Thannoun, R., Al-Kubaisi, M., Al-Hasani, B., Abdellatif, M., and Carnacina, I., 2025. Classifying Fluvial Landforms Using Geospatial Modeling in Al-Ashaali Watershed, Iraqi Southern Desert. Bulletin Of the Iraq Natural History Museum, 18(3), 739–763. https://doi.org/10.26842/binhm.7.2025.18.3.0739

Mahala, A., 2020. The significance of morphometric analysis to understand the hydrological and morphological characteristics in two different morpho-climatic settings. Applied Water Science, 10(1). https://doi.org/10.1007/s13201-019-1118-2

Minár, J., Drăguţ, L., Evans, I.S., Feciskanin, R., Gallay, M., Jenčo, M., and Popov, A., 2024. Physical geomorphometry for elementary land surface segmentation and digital

geomorphological mapping. In Earth-Science Reviews (Vol. 248). Elsevier B.V. https://doi.org/10.1016/j.earscirev.2023.104631

Morisawa, M., 1989. Rivers and valleys of Pennsylvania, revisited. Geomorphology, 2(1–3), 1–22. https://doi.org/10.1016/0169-555X(89)90003-2

MR, R.C.B. and Achyuthan, H., 2019. Quantitative analysis of the drainage and morphometric characteristics of the Palar River basin, Southern Peninsular India; using bAd calculator (bearing azimuth and drainage) and GIS. Geology, Ecology, and Landscapes, 3(4), 295–307. https://doi.org/10.1080/24749508.2018.1563750

Newman, D.R., Cockburn, J.M.H., Drăguţ, L. and Lindsay, J.B., 2022. Evaluating Scaling Frameworks for Multiscale Geomorphometric Analysis. Geomatics, 2(1), 36–51. https://doi.org/10.3390/geomatics2010003

Niculiță, M., 2020. Geomorphometric methods for burial mound recognition and extraction from high-resolution LiDAR DEMs. Sensors (Switzerland), 20(4). https://doi.org/10.3390/s20041192

Pinto, F.M., Schuch, F.S., and Brentano, D.M., 2023. Extreme precipitation events and geomorphic adjustments in the riverscape: A case study in Southern Brazil. Resources, Environment and Sustainability, 13. https://doi.org/10.1016/j.resenv.2023.100124

Prasannakumar, V., Shiny, R., Geetha, N., and Vijith, H., 2011. Applicability of SRTM data for landform characterisation and geomorphometry: A comparison with contour-derived parameters. International Journal of Digital Earth, 4(5), 387–401. https://doi.org/10.1080/17538947.2010.514010

Rai, P.K., Chandel, R.S., Mishra, V.N., and Singh, P., 2018. Hydrological inferences through morphometric analysis of lower Kosi River basin of India for water resource management based on remote sensing data. Applied Water Science, 8(1). https://doi.org/10.1007/s13201-018-0660-7

Şarlak, N. and Mahmood Agha, O.M.A., 2018. Spatial and temporal variations of aridity indices in Iraq. Theoretical and Applied Climatology, 133(1–2), 89–99. https://doi.org/10.1007/s00704-017-2163-0

Sissakian, V.K. and Fouad, S.F.A., 2015. Geological Map of Iraq, Scale 1: 1000 000, 4 Th Edition, 2012. In Iraqi Bulletin of Geology and Mining (Vol. 11, Issue 1).

Smith, K.G., 1950. Standards for grading texture of erosional topography. American Journal of Science, 248(9), 655–668. https://doi.org/10.2475/ajs.248.9.655

Stanley A.S., 1956. Evolution Of Drainage Systems and Slopes in Badlands at Perth Amboy, New Jersey. Gsa Bulletin, 67(5), pp. 597–646.

Strahler, A.N., 1954. Statistical Analysis in Geomorphic Research. The Journal Of Geology, 62(1), 1–25. https://doi.org/https://doi.org/10.1086/626131

Strahler, A.N., 1957. Quantitative Analysis of Watershed Geomorphology. Transactions, American Geophysical Union, 38(6), 913–920.

Vörös, F., van Wyk de Vries, B., Guilbaud, M.N., Görüm, T., Karátson, D., and Székely, B., 2022. DTM-Based Comparative Geomorphometric Analysis of Four Scoria Cone Areas—Suggestions for Additional Approaches. Remote Sensing, 14(23). https://doi.org/10.3390/rs14236152

Zhou, A., Chen, Y., Wilson, J.P., Chen, G., Min, W., and Xu, R., 2023. A multi-terrain feature-based deep convolutional neural network for constructing super-resolution DEMs. International Journal of Applied Earth Observation and Geoinformation, 120. https://doi.org/10.1016/j.jag.2023.103338